

Proceedings of the 13th International Newborn Brain Conference: Neuro-imaging studies

Virtual conference, February 10th-12th 2022

Ramy Abramsky, Rebeka Acosta, Laura Acosta Izquierdo, Bushra Albeshri, Mountasser Almouqdad, Yasmeen Asfour, Suzan Asfour, Topun Austin, Ashley Bach, Jim Barkovich, Richard Beare, Nadya Ben Fadel, Angelika Berger, Borja Blanco, Martijn Boomsma, Samudragupta Bora, Vivian Boswinkel, Theresa Chin, Liam Collins-Jones, Robert Cooper, Gautam Dagur, Jorge Davila, Linda de Vries, Laxmikant Shesrao, Deshmukh, Gregor Dovjak, Andrea Edwards, Mohamed El-Dib, Hoda Elshibiny, Dafna Eshel, Ron Eshel, Donna Ferriero, Dawn Gano, Olivia Girvan, Hannah Glass, Katharina Goral, Agneta Golan, Michelle Gurvitz, Terrie Inder, Dima Jamjoom, Nadja Kadom, Gregor Kasprian, Thanaa Khalil, Katrin Klebermass-Schrehof, Jake Kleinmahon, Martine Krüse-Ruijter, Hannah Lambing, Sarah Lee, Alexander Leemans, Lara Leijser, Brigitte Lemyre, Yi Li, Camille Maltais-Bilodeau, Kyla Marks, Charles McCulloch, Sarah Milla, Elka Miller, Aradhana Mishra, Nicholas Mitsakakis, Khorshid Mohammad, Susanne Mulder-de Tollenaer, Chelsea Munster, Jacqueline Nijboer, Jacqueline Nijboer-Oosterveld, Ingrid Nijholt, Rosa Novoa, Cynthia Ortinou, Emma Porter, Daniela Prayer, Deepti Reddy, Stephanie Redpath, Elizabeth Rogers, Victor Schmidbauer, James Scott, Elizabeth Sewell, Eilon Shany, Ilan Shelef, Elizabeth Singh, Cornelis Slump, Tina Steele, Eniko Szakmar, Chantal Tax, Kirsten Thiim, Julie Uchitel, Jochen van Osch, Gerda van Wezel-Meijler, Anouk Verschuur, Mei-Nga Wu-Smit, Edward Yang, Hussein Zein.

Association between anterior cerebral artery resistive index on ultrasound, brain injury on MRI, and outcome in newborns who received therapeutic hypothermia

Acosta L^a, Maltais-Bilodeau C^a, Reddy D^a, Mitsakakis N^a, Davila J^a, Lemyre B^a, Ben Fadel N^a, Redpath S^a, Miller E^a

^a*CHEO, University of Ottawa, Ottawa, Canada*

BACKGROUND/PURPOSE: Therapeutic hypothermia (TH) initiated within the first 6 hours after birth, is proven to decrease brain tissue injury in moderate to severe neonatal encephalopathy (NE) and improve 18-24 month neurological outcomes. Recently, a correlation between the resistive index (RI) of the anterior cerebral artery on head ultrasound (HUS) performed after rewarming and severity of injury on MRI was reported. It remains unknown whether early RI anomalies (before rewarming) may be associated with severity of injury on MRI and as such, might have prognostic value for infants too unstable to undergo an MRI within the optimal time window. The aim of this study was to evaluate: (i) the association between a low anterior cerebral artery RI on HUS obtained during active TH and the severity of brain injury on MRI, and to examine the association between the RI value and outcomes at 48 months of age.

METHODOLOGY: A retrospective study was performed. Electronic patient data records and patient charts were reviewed to identify infants born ≥ 35 weeks of gestation between October 2009 and December 2016, who received TH, at the Children's Hospital of Eastern Ontario. RI on HUS in the first three days of life were compared to brain MRI findings based on the scoring system by Weeke et al. Outcomes at 48 months of life were based on the Ages and Stages questionnaire administered during a clinic visit.

RESULTS: Of the 101 newborns (median 39 weeks (IQR 38, 40); median birth weight 3.4 kg (IQR 3.0-3.8)) who underwent TH, 74 had doppler ultrasound of the anterior cerebral artery. The median age at which TH was achieved was 5.8 hours of life (IQR = 4.0 – 8.1). The median (IQR) for time to first ultrasound was 16.5 (10.7-24.3) hours. The mean RI in the initial ultrasound was 0.65 (IQR 0.59 – 0.73). 62 newborns had brain MRI, with a median of the total Weeke score of 2.5 (IQR = 0 – 11); the median grey matter score was 0 (IQR 0.0 – 4.0). Overall, there is little to no correlation between the mean RI and total Weeke score. There is a weak negative correlation between the mean RI and the Weeke grey matter score (Pearson(95% CI): -0.37 (-0.57–0.13; p-value=0.05). The logistic regression model, did not show any significant association between mean RI and neurologic outcome at 48 months (p=0.39).

CONCLUSION: Despite the small sample size of the study cohort, the mean RI of the anterior cerebral artery shows some degree of correlation with the Weeke grey matter score on MRI. This suggests it may be helpful as a

biomarker in neonates with encephalopathy under TH, especially those that are severely compromise where an MRI may be unsafe.

Association between morphine exposure and brain injury on term-equivalent age brain magnetic resonance imaging in very preterm infants

Almouqdad M^a, Jamjoom D^b, Khalil T^a, Asfour Y^c, Albeshri B^a, Asfour S^a

^aKing Saud medical city, Riyadh, Saudi Arabia

^bKing Saud University, Riyadh, Saudi Arabia

^cFamily Care Hospital, Riyadh, Saudi Arabia

OBJECTIVE: To investigate the relationship between morphine exposure in the first week of life and brain injury on term-equivalent age magnetic resonance imaging (MRI) in very preterm infants.

METHODS: We included 106 infants with a birth weight of < 1500 g who were born at King Saud Medical City at ≤ 32 gestational weeks, were admitted to the neonatal intensive care unit, and underwent term-equivalent age and pre-discharge brain MRI. Modified log-Poisson regression with a robust variance estimator was applied, and the effect of early morphine exposure on brain morphology and growth at term-equivalent age was determined using the Kidokoro score.

RESULTS: Sixty-eight (64.2%) infants had received morphine in the first week of life (median cumulative dose: 1.68 mg/kg, interquartile range: 0.48–2.52 mg/kg). Early initiation of morphine administration was significantly associated with high total white matter

(adjusted relative risk [aRR]: 1.32, 95% confidence interval [CI]: 1.01–1.72) and cerebellum (aRR: 1.36, 95% CI: 1.03–1.81) scores and a low cerebellar volume (aRR: 1.28, 95% CI: 1.02–1.61).

CONCLUSION: Morphine exposure in the first week of life was independently associated with white matter and cerebellar injury on term-equivalent age brain MRI in very preterm infants.

Bibliography:

- [1] Smith, G.C. et al. Neonatal intensive care unit stress is associated with brain development in preterm infants. *Ann. Neurol.* 70, 541-549 (2011).
- [2] Kumar, P., Walker, J.K., Hurt, K.M., Bennett, K.M., Grosshans, N. & Fotis, M.A. Medication use in the neonatal intensive care unit: current patterns and off-label use of parenteral medications. *J. Pediatr.* 152, 412-415 (2008).
- [3] Anand, K.J. et al. Effects of morphine analgesia in ventilated preterm neonates: primary outcomes from the NEOPAIN randomised trial. *Lancet* 363,1673-1682 (2004).
- [4] Steinhorn, R., McPherson, C., Anderson, P.J., Neil, J., Doyle, L.W. & Inder, T. Neonatal morphine exposure in very preterm infants-cerebral development and outcomes. *J. Pediatr.* 166, 1200-1207 (2015).
- [5] Zwicker, J.G. et al. Smaller Cerebellar Growth and Poorer Neurodevelopmental Outcomes in Very Preterm Infants Exposed to Neonatal Morphine. *J. Pediatr.* 172, 81-87 (2016).
- [6] Ranger, M. et al. Neonatal Pain and Infection Relate to Smaller Cerebellum in Very Preterm Children at School Age. *J. Pediatr.* 167, 292-298 (2015).

Table 1. Univariate analysis of global brain abnormalities score on TEA-MRI in relation to morphine exposure in first week of life (n=106)

	Exposure to morphine in the first 7 days of life		p value
	No (38)	yes (68)	
White matter score			
Cystic lesions	0 (0-3)	0 (0-3)	0.13
Focal signal abnormality	0 (0-0.25)	0 (0-2)	0.02*
Myelination delay	1 (1-1)	1 (1-2)	0.06
Thinning of the corpus callosum	0 (0-0.25)	0 (0-2)	0.009*
Dilated lateral ventricles	0 (0-1)	2 (0-3)	0.004*
Volume reduction	1.5 (1-2)	2 (1-2)	0.14
Total white matter score	3 (2-8)	7 (4-11)	<0.001*
Cortical gray matter score			
Signal abnormality	0 (0-0)	0 (0-0)	0.38
Gyral maturation	0 (0-0)	0 (0-0)	0.71
Increased extracerebral space	0 (0-0)	0 (0-0)	0.09
Total cortical gray matter score	0 (0-0.25)	0 (0-1)	0.59
Deep gray matter score			
Signal abnormality	0 (0-0)	0 (0-1)	0.06
Volume reduction	0 (0-0)	0 (0-2)	0.01*
Total deep gray matter score	0 (0-0.25)	0 (0-3)	0.01*
Cerebellum score			
Signal abnormality	0 (0-0)	0.5 (0-3)	0.001*
Volume reduction	1 (1-2)	3 (1-3)	<0.001*
Total cerebellar score	1 (1-3)	3 (2-5)	<0.001*
Global brain abnormality score	5.5 (3.75-14)	11.5 (8-19)	<0.001*

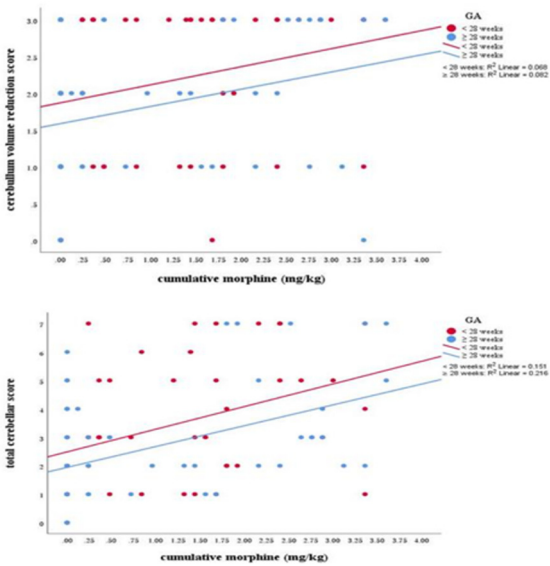
Data are presented as median (IQR), or number (%), as appropriate.

*Statistically significant at 5% level

Table 2. Multivariable regression of global brain abnormalities score on TEA-MRI in relation to morphine exposure in first week of life (n=106)

Outcome	aRR	95% CI	P value
White matter score			
Focal signal abnormality	0.68	0.31-1.49	0.33
Thinning of the corpus callosum	1.1	0.52-2.31	0.79
Dilated lateral ventricles	1.01	0.6-1.71	0.95
Total white matter score	1.32	1.01-1.72	0.03*
Deep gray matter score			
Volume reduction	0.91	0.42-1.94	0.79
Total deep gray matter score	1.11	0.48-2.58	0.8
Cerebellum score			
Signal abnormality	1.19	0.51-2.79	0.67
Volume reduction	1.28	1.02-1.61	0.02*
Total cerebellar score	1.36	1.03-1.81	0.02*
Global brain abnormality score	1.31	0.99-1.74	0.06

Abbreviations: *aRR* adjusted relative risk, *CI* Confidence interval
 *Statistically significant at 5% level



- [7] Simons, S.H. et al. Routine morphine infusion in preterm newborns who received ventilatory support: a randomized controlled trial. *JAMA* 290, 2419-2427 (2003).
- [8] de Graaf, J. et al. Does neonatal morphine use affect neuropsychological outcomes at 8 to 9 years of age? *Pain* 154, 449-458 (2013).
- [9] van den Bosch, G.E. et al. Prematurity, Opioid Exposure and Neonatal Pain: Do They Affect the Developing Brain? *Neonatology* 108, 8-15 (2015).
- [10] Miller, S.P. et al. Early brain injury in premature newborns detected with magnetic resonance imaging is associated with adverse early neurodevelopmental outcome. *J. Pediatr.* 147, 609-616 (2005).

Prenatal cerebral abnormalities in congenital heart disease detected on structural magnetic resonance imaging

Dagur G^{a,b}, Ortinau C^c, Chin T^a, Kleinmahon J^{b,d}, Gurvitz M^{e,f}, Bora S^f

^a*Mothers, Babies and Women’s Health, Mater Research Institute, Faculty of Medicine, The University of Queensland, Brisbane, Australia*
^b*Ochsner Clinical School, Faculty of Medicine, The University of Queensland, New Orleans, United States*
^c*Pediatrics, Washington University School of Medicine, St. Louis, United States*
^d*Pediatric Cardiology, Ochsner Hospital for Children, New Orleans, United States*
^e*Pediatrics, Harvard Medical School, Boston, United States*

^fCardiology, Boston Children’s Hospital, Boston, United States

BACKGROUND: Fetuses with congenital heart disease (CHD) are vulnerable to alterations of the developing brain.¹ Despite growing recognition of prenatal cerebral abnormalities, there is limited understanding primarily due to small sample sizes and varying neuroimaging modalities.^{2,3} The aim of this study was to conduct a systematic review and meta-analysis, appraising evidence to estimate the prevalence of prenatal cerebral abnormalities in CHD detected on magnetic resonance imaging (MRI).

METHODOLOGY: This study was conducted according to the Preferred Reporting Items for Systematic reviews and Meta-Analyses guideline. Two independent reviewers screened five electronic databases (CINAHL, EMBASE, PsycINFO, PubMed/MEDLINE, and SCOPUS) using combinations of MeSH terms and keywords in the format of population, exposure, outcome, and neuroimaging modality to identify peer-reviewed English language publications from inception to February 2021. Inclusion criteria were: 1) sample aged 24 weeks gestation to birth, with 2) isolated (non-syndromic) CHD, reporting 3) prenatal cerebral abnormalities on structural MRI, and using 4) cohort, case-control, or cross-sectional study designs. CHD subtypes and cerebral abnormalities were classified as reported in the original studies. Studies were excluded if they reported 1) outcomes on neuroimaging modalities other than MRI, or 2) structural MRI measures (e.g., volumetrics and surface-based analyses) without rates of abnormalities. For studies reporting outcomes of the same cases, the study with the largest sample size was included in the meta-analysis, to ensure sample independence. Random-effects modeling was used for pooled prevalence estimates and heterogeneity based on I².

Figure 1. PRISMA flowchart for study selection.

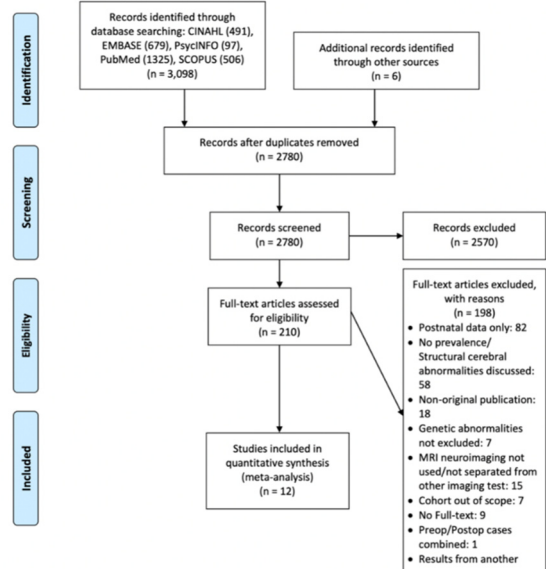
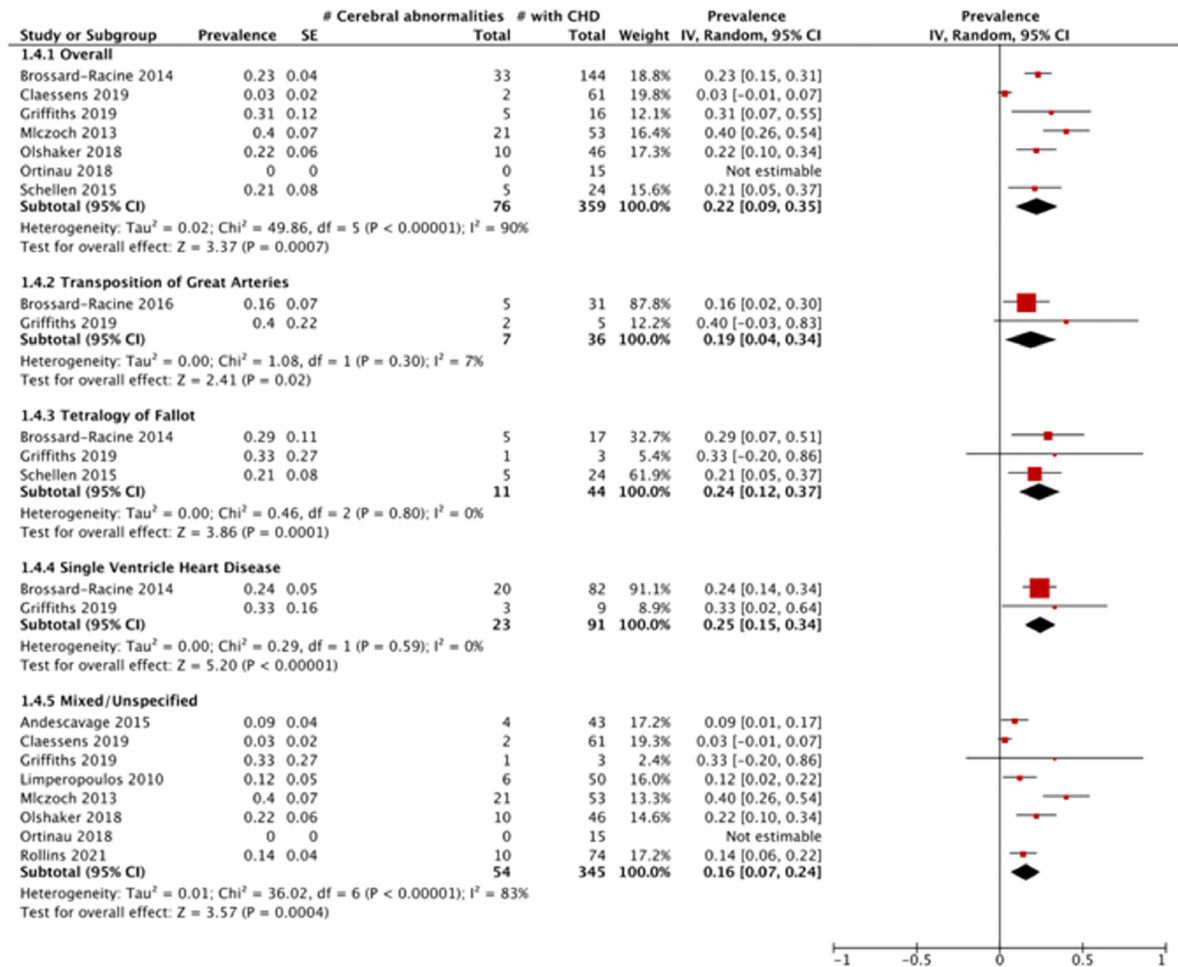


Figure 2. Prevalence of prenatal cerebral abnormalities in congenital heart disease.**Table 1.** Characteristics of studies included in the systematic review and meta-analysis.

First Author, Year	Country; Year of Birth	Male, %	MRI Strength, Tesla	Age at MRI, Gestational Weeks	CHD Subtypes	Fetuses with Cerebral Abnormalities	Fetuses with MRI	Study Quality Rating
Andescavage, 2015	USA; NR	67	1.5	31 (4) ^a	Mixed/Unspecified	4	43	High
Brossard-Racine, 2016	USA; 2007–2010, 2011–2014	NR	1.5 or 3.0	32 (4) ^a	TGA, ToF, SVHD, Mixed/Unspecified	17	103	High
Brossard-Racine, 2014	USA; 2007–2013	57	1.5	31 (5) ^a	TGA, ToF, SVHD, Mixed/Unspecified	33	144	High
Claessens, 2019	The Netherlands; 2016–2017	70	3.0	33 (33–34) ^e	Mixed/Unspecified	2	61	High
Clouchoux, 2013	USA; 2007–2008	61	1.5	30 (25–37) ^b	SVHD	5	18	Moderate
Griffiths, 2019	United Kingdom; NR	NR	1.5	28–36 ^c	TGA, ToF, SVHD, Mixed/Unspecified	5	16	Moderate
Limperopoulos, 2010	USA; 2007–2008	64	1.5	31 (25–36) ^b	Mixed/Unspecified	6	50	Moderate
Mlczoch, 2013	Austria; 2002–2008	NR	1.5	28 (20–37) ^d	Mixed/Unspecified	21	53	High
Olshaker, 2018	Israel; 2011–2014	59	1.5	32 (32–34) ^e	Mixed/Unspecified	10	46	Moderate
Ortinou, 2018	USA; 2012–2015	NR	1.5	33 (3) ^a	Mixed/Unspecified	0	15	High
Rollins, 2021	USA; 2014–2018	64	3.0	NR	Mixed/Unspecified	10	74	High
Schellen, 2015	Austria; 2004–2014	NR	1.5	25 (20–34) ^b	ToF	5	24	High

Abbreviations: MRI, magnetic resonance imaging; CHD, congenital heart disease; TGA, transposition of great arteries; ToF, tetralogy of fallot; SVHD, single ventricle heart disease; NR, not reported.

^a Mean (Standard Deviation); ^b Median (Range); ^c Range; ^d Mean (Range); ^e Median (Interquartile Range).

Mixed/Unspecified CHD subtype includes all other subtypes not included in TGA, ToF, or SVHD.

RESULTS: As shown in Figure 1, the systematic search yielded 12 studies fulfilling the inclusion criteria, comprising 435 fetuses with isolated CHD. Study characteristics are summarized in Table 1. As shown in Figure 2, the overall prevalence of prenatal cerebral abnormalities in CHD detected on structural MRI was 22% (95% CI=9%–35%), with 25% in single ventricle heart disease, 24% tetralogy of fallot, 19% in transposition of great arteries, and 16% in mixed/unspecified lesions.

CONCLUSION: Findings provide evidence that CHD is associated with prenatal cerebral abnormalities, with more than a fifth of this high-risk population at risk. Further studies are warranted to better understand the longitudinal progression of these abnormalities and their association with neurodevelopmental outcomes. This study was limited by reliance on cerebral abnormalities as defined in the original studies, thereby resulting in a heterogeneous profile of prenatal cerebral injuries and/or alterations.

Bibliography:

- [1] Bonthron AF, et al. MRI studies of brain size and growth in individuals with congenital heart disease. *Translational Pediatrics*. 2021;10(8):2171-2181.
- [2] Jansen FA, et al. Fetal brain imaging in isolated congenital heart defects – a systematic review and meta-analysis. *Prenatal Diagnosis*. 2016;36(7):601-613.
- [3] Khalil A, et al. Prevalence of prenatal brain abnormalities in fetuses with congenital heart disease: a systematic review. *Ultrasound in Obstetrics & Gynecology*. 2016;48(3):296-307.

Facilitators and barriers of neuroimaging in children with congenital heart disease

Dagur G^{a,b}, Kleinmahon J^{b,c}, Gurvitz M^{d,e}, Acosta R^f, Bora S^a

^a*Mothers, Babies and Women's Health, Mater Research Institute, Faculty of Medicine, The University of Queensland, Brisbane, Australia*

^b*Ochsner Clinical School, Faculty of Medicine, The University of Queensland, New Orleans, United States*

^c*Pediatric Cardiology, Ochsner Hospital for Children, New Orleans, United States*

^d*Pediatrics, Harvard Medical School, Boston, United States*

^e*Cardiology, Boston Children's Hospital, Boston, United States*

^f*On Behalf of Conquering CHD, United States*

BACKGROUND: There has been increasing recognition of the prognostic utility of neuroimaging in high-risk pediatric neurodevelopment.^{1,2} It is now well-documented

that brain injuries or abnormalities are associated with neurodevelopmental delays/deficits in children with congenital heart disease (CHD).³ Thus, the aim of this study was to identify the facilitators and barriers to attending pediatric neuroimaging, as reported by primary caregivers of children with CHD.

METHODOLOGY: As part of a cross-sectional study, 409 primary caregivers of children with CHD residing in the U.S. completed an online survey, with 108 and 301 children with and without neuroimaging for CHD, respectively. The survey was disseminated between November 2020 and January 2021. Sample recruitment was facilitated by Conquering CHD, the largest CHD patient and family advocacy organization in the U.S. Responses of participants regarding facilitators and barriers to attending neuroimaging were classified into 15 categories. Further, these were stratified into three themes corresponding to healthcare systems, health care professionals, and primary caregivers.

RESULTS: A descriptive profile of child clinical and family sociodemographic characteristics is provided in Table 1. Relative to children without neuroimaging, those with neuroimaging had significantly higher rates of antenatal CHD diagnosis (50% vs. 62%), single ventricle physiology (28% vs. 43%), and extended first ICU stay (37% vs. 51%). Further, 34% of children without neuroimaging, compared with 25% of children with neuroimaging, were living ≥ 60 miles from the nearest pediatric cardiology center. As shown in Figure 1a–c, factors related to primary caregivers and health care professionals were the most common determinants of neuroimaging for children with CHD. Among those who

Table 1. Child clinical and family sociodemographic characteristics of the sample with and without neuroimaging for children with congenital heart disease.

Characteristic, % (n/N)	With Neuroimaging, N=108	Without Neuroimaging, N=301	p	Total sample, N=409
Child clinical				
Male sex	55 (59/108)	59 (176/301)	.49	58 (235/409)
Preterm birth [<37 weeks gestation]	14 (15/107)	20 (59/298)	.18	18 (74/405)
Antenatal CHD diagnosis	62 (67/108)	50 (149/300)	.03	53 (216/408)
Single ventricle physiology	43 (46/108)	28 (83/301)	.004	32 (129/409)
Open heart surgery	94 (102/108)	88 (264/300)	.06	90 (366/408)
Heart transplant	3 (3/108)	2 (7/300)	.80	3 (10/408)
Extracorporeal membrane oxygenation	28 (28/101)	25 (65/263)	.56	26 (93/364)
Extended first ICU stay [>21 days]	51 (55/107)	37 (109/298)	.007	41 (164/405)
Prenatal neuroimaging scan	8 (9/108)	-	-	-
Neuroimaging modality				
Computed tomography	44 (48/108)	-	-	-
Magnetic resonance imaging	69 (75/108)	-	-	-
Ultrasound	41 (44/108)	-	-	-
Biological maternal [childbirth]				
Young motherhood [<25 years]	9 (10/108)	15 (45/293)	.12	14 (55/401)
Single motherhood	6 (6/108)	6 (19/301)	.78	6 (25/409)
Minority race	8 (9/107)	9 (26/298)	.92	9 (35/405)
Low academic attainment	6 (6/108)	7 (22/301)	.54	7 (28/409)
Family social background [concurrent]				
Public health insurance	24 (30/108)	28 (71/301)	.39	25 (101/409)
Low socioeconomic status [$<US\$30,000$ per annum]	12 (13/108)	17 (50/301)	.26	15 (63/409)
Distant proximity to pediatric cardiology service [≥ 60 miles] ^a	25 (27/108)	34 (102/301)	.09	32 (129/409)
U.S. geographical region residence				
Northeast	13 (14/108)	13 (39/301)	.61	13 (53/409)
Midwest	37 (40/108)	36 (109/301)	.36	36 (149/409)
South	34 (37/108)	30 (89/301)	.31	31 (126/409)
West	16 (17/108)	21 (64/301)	.20	21 (81/409)

Abbreviations: CHD, congenital heart disease; ICU, intensive care unit.

^aPediatric cardiology service at a free-standing children's hospital or larger hospital/healthcare organization with/without academic affiliation.

underwent neuroimaging, the biggest facilitator was the perceived benefits of neuroimaging by primary caregivers, reported by 67% of respondents. Further, 63% indicated the importance of health care professionals' communication regarding neuroimaging as a major facilitator. Correspondingly, for children without neuroimaging, the biggest reported barriers were health care professionals' communication (79%) and limited understanding of the primary caregiver (54%) concerning neuroimaging.

CONCLUSION: To facilitate increased uptake of neuroimaging, study findings highlight the need to enhance awareness and knowledge of primary caregivers regarding the utility of neuroimaging for children with CHD. Further, the critical role of health care providers' communication is emphasized, particularly highlighting the importance of neuroimaging in relation to neurodevelopmental outcomes. Taken together, a multifactorial approach is required to support follow-up care of children with CHD and their families.

Bibliography:

- [1] Guillot M, et al. Comparative performance of head ultrasound and MRI in detecting preterm brain injury and predicting outcomes: A systematic review. *Acta Paediatrica*. 2021;110(5):1425-1432.
- [2] Ouwehand S, et al. Predictors of outcomes in hypoxic-ischemic encephalopathy following hypothermia: A meta-analysis. *Neonatology*. 2020;117(4):411-427.
- [3] Mebius MJ, et al. Brain injury and neurodevelopmental outcome in congenital heart disease: A systematic review. *Pediatrics*. 2017;140(1):e20164055.

Conventional neonatal MRI predicts gross motor disability at four years in children with neonatal encephalopathy

Lambing H^a, Gano D^a, Li Y^a, Bach A^b, Girvan O^c, Rogers E^a, Ferriero D^a, Barkovich J^a, McCulloch C^a, Glass H^a

^aUniversity Of California, San Francisco, San Francisco, United States

^bChildren's Hospital of Philadelphia, Philadelphia, United States

^cJohns Hopkins University, Baltimore, United States

BACKGROUND: Children with neonatal encephalopathy due to hypoxic-ischemic encephalopathy are at risk for basal ganglia/thalamus (BG/T) and watershed (WS) patterns of brain injury. We previously showed that neuromotor impairment at 30 months of age is more common in infants with BG/T than with WS injury [Miller S.P., 2005]. The relationship between neonatal imaging and early childhood outcome is not well characterized.

METHODS: Term neonates at risk for brain injury due to neonatal encephalopathy were prospectively enrolled at UCSF Benioff Children's Hospital from 1993-2014 and received MRI within two weeks after birth. A neuroradiologist blinded to clinical condition scored brain injury in the BG/T pattern (from 0, no injury to the deep gray nuclei, to 4, basal ganglia, thalamic, perirolandic and additional cortical injury) [Barkovich A.J., 1998]. Brain injury was quantified as a full-scale (no injury, WS injury only, and BG/T scores 1-4) and dichotomized BG/T (0-1 vs. 2-4). Two researchers independently assigned a Gross Motor Function Classification System (GMFCS) score for cerebral palsy (CP) at age four years based on a structured neurological examination (linearly weighted kappa=0.881). To describe the predictive value of the MRI, the relationship between BG/T injury and dichotomized GMFCS (0-2=none/mild vs. 3-5=moderate/severe CP) was evaluated with logistic regression. Covariates associated with injury were added stepwise to the model and cross-validated AUROC was used to determine the model with the best predictive performance.

RESULTS: Of the 408 newborns enrolled and imaged, 356 (93%) survived and 174 (49%) of survivors attended the four-year follow-up (Figure 1). MRI at a median age of 4 days (IQR 3-6) showed no injury in 65 (38%), WS injury only in 56 (32%), and BG/T injury of varying severity in 53 (31%, Table 1). At four years (50 +/- 5 months), 145 children (83%) had no CP, 18 children (10%) had mild CP (GMFCS=1-2), and 11 children (6%) had moderate-severe CP (GMFCS=3-5). Higher BG/T scores were associated with higher GMFCS (Figure 2). Both the binary and full-scale predictor had high AUROC (0.8865 and 0.8945, respectively); clinical covariates did not meaningfully add to the model. Risk of moderate-severe CP was low (<20%)

Figure 1. Facilitators and barriers of neuroimaging in children with congenital heart disease. a) Healthcare system factors. b) Health care professional factors. c) Primary caregiver factors.

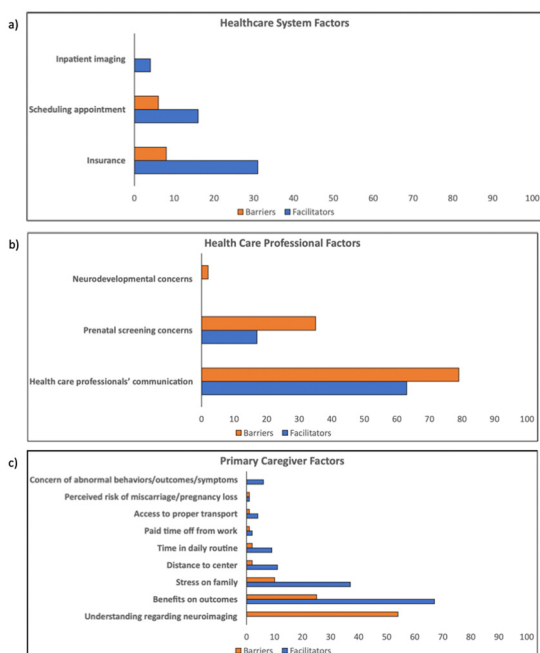
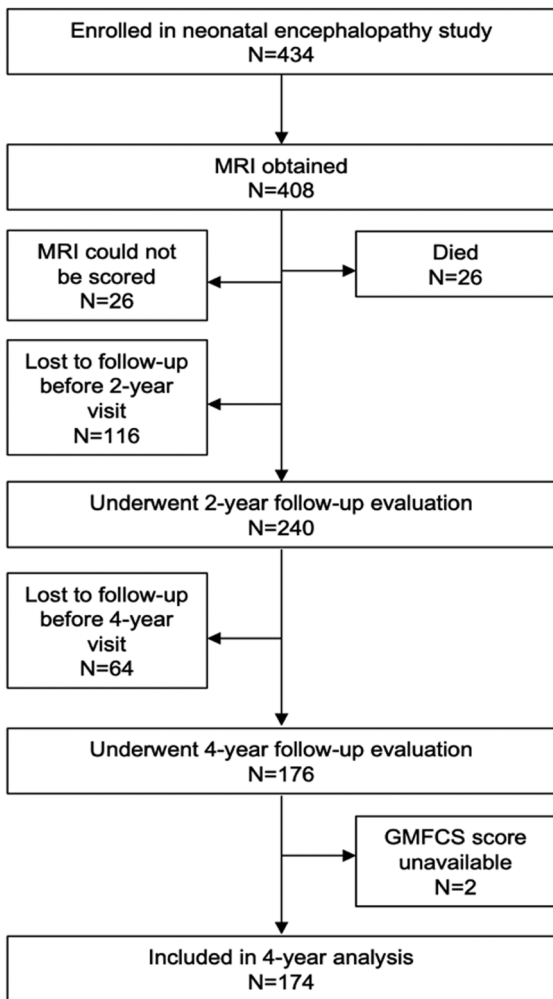


Table 1: Newborn clinical characteristics among 174 children with neonatal encephalopathy

Characteristics	No injury (BG/T=0, WS=0)	Watershed injury (BG/T=0, WS=1-5)	Abnormal signal in the thalamus (BG/T=1)	Abnormal signal in the thalamus and lentiform nucleus (BG/T=2)	Abnormal signal in the thalamus, lentiform nucleus, and perioral cortex (BG/T=3)	More extensive involvement (BG/T=4)	P-value
N	65	56	14	18	12	9	
Male	30 (46%)	34 (61%)	8 (57%)	12 (67%)	7 (58%)	3 (33%)	0.36
Race/Ethnicity							0.49
BIPOC	18 (28%)	11 (20%)	5 (36%)	7 (39%)	5 (42%)	5 (56%)	
White, non-Hispanic	47 (72%)	44 (79%)	9 (64%)	11 (61%)	7 (58%)	4 (44%)	
Unknown	0 (0%)	1 (2%)	0 (0%)	0 (0%)	0 (0%)	0 (0%)	
Caesarean section	36 (55%)	31 (55%)	5 (36%)	8 (44%)	5 (42%)	6 (67%)	0.59
Gestational Age, mean (SD)	40 (1.3)	39 (1.8)	39 (2)	39 (1.5)	41 (.85)	40 (2.2)	0.010
Birthweight (g), mean (SD)	3,485 (540)	3,278 (505)	3,041 (839)	3,252 (445)	3,401 (438)	3,233 (890)	0.088
APGAR at 5 minutes, median (IQR)	5 (3, 7)	5 (3, 6)	4 (3, 5)	3 (3, 6)	4 (3, 6.5)	4 (3, 5)	0.33
Therapeutic Hypothermia	34 (52%)	17 (30%)	4 (29%)	1 (6%)	1 (8%)	1 (11%)	<0.001

BIPOC = Black, Indigenous, and People of Color; BG/T = Basal Ganglia/Thalamus; WS = Watershed; SD = Standard Deviation; IQR = Interquartile Range

Figure 1: Flow diagram of study participants.



in all patterns of brain injury except BG/T=4, which carried 67% probability (95% CI 36-98%) of moderate-severe CP (Figure 3).

Figure 2: Violin Plot of gross motor function classification score (GMFCS) at age four years by basal ganglia/thalamus (BG/T) injury severity at birth. Black dot indicates median score.

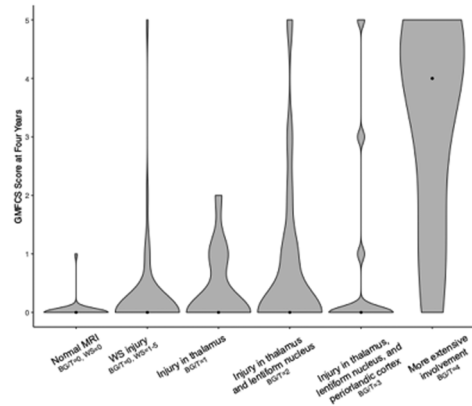
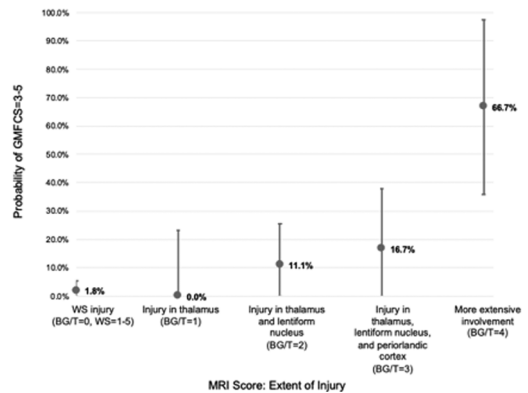


Figure 3: Predictive probability of moderate-severe cerebral palsy (GMFCS=3-5) with 95% confidence intervals by pattern of brain injury.



CONCLUSIONS: In this large, prospective cohort of children with neonatal encephalopathy, the risk of moderate-severe CP was very low, particularly for children with BG/T=0-3. However, among children with BG/T=4, two-thirds had moderate-severe CP indicating inability to

ambulate independently at age four years. Understanding the relationship between neonatal MRI and motor outcome is important for clinicians to provide recommendations for treatment and resources to families at the time of birth and diagnosis, rather than when the motor abnormalities become apparent in early childhood.

Effectiveness of the Canadian consensus approach for diagnosis and grading of preterm brain injury from cranial Ultrasound

Leijser L^a, Scott J^b, Zein H^a, Mohammad K^a

^aUniversity of Calgary, Cumming School of Medicine, Department of Pediatrics, Section of Neonatology, Calgary, Canada

^bUniversity of Calgary, Cumming School of Medicine, Department of Radiology, Calgary, Canada

BACKGROUND AND PURPOSE: Cranial ultrasound (cUS) is the first-line tool to screen the vulnerable preterm infant's brain for injury. Concerns, however, remain regarding variability in diagnosis and grading of common preterm brain injury types from cUS between Neonatologists and Radiologists within and across neonatal centers. We recently developed a Canadian consensus approach to decrease this variability.¹ The current study assessed the interobserver agreement in diagnosis and grading of preterm brain injury from cUS before and after the implementation of the consensus approach in our centers.

METHODS: Retrospective observational study in extremely preterm infants (<29 weeks) who were admitted to Calgary neonatal centers between 2010-2019 and had ≥ 3 cUS scans throughout the neonatal period. All available serial cUS scans were assessed by a Neonatologist and Radiologist before and after implementation of the consensus approach. Assessments included: Presence and grade (1 to 3) of germinal matrix-intraventricular hemorrhage (GMH-IVH; with grade 3 defined as IVH with anterior horn width of lateral ventricle >6mm), and associated presence of periventricular hemorrhagic infarction (PVHI), post-hemorrhagic ventricular dilatation (PHVD; defined as enlarged ventricular measurements on repeated scans), cystic white matter injury (cWMI) and cerebellar hemorrhage (CBH). Interobserver agreement (intra-class correlation coefficient [ICC]) after consensus approach implementation was tested for all injury types. In addition, ICCs before and after implementation were compared for GMH-IVH presence and grading. In case of inconsistency in observers' assessment, consensus on injury diagnosis and grading was reached through case discussion.

RESULTS: As per consensus, 292 out of 1452 (20%) eligible infants showed unilateral or bilateral GMH-IVH,

with a total of 460 GMH-IVHs diagnosed among these infants (Table). Interobserver agreement for GMH-IVH presence and grading was good (ICC 0.85) before, while excellent (ICC 0.93) after consensus approach implementation. Of the 33 (7%) inconsistencies between observers in GMH-IVH grading, only four (0.9%) involved a grade 3 IVH, of potential clinical significance. Among the 292 infants, associated PVHI, PHVD, cWMI and/or CBH was diagnosed in 88 (30%), 65 (22%), 7 (2%) and 8 (3%) infants, respectively. Interobserver agreement after implementation was excellent (ICC ≥ 0.92) for all these injury types (Table).

CONCLUSIONS: Our study shows that the development of a consensus approach facilitates a high consistency in diagnosis and grading of common and clinically significant brain injury types from cUS in extremely preterm infants. The consensus approach may contribute to better identification of risk factors for preterm brain injury and therewith improved clinical care. Also, it has the potential of improving prediction of long-term neurodevelopmental outcomes of preterm infants from serial cUS. Further study to this end is required.

Bibliography:

- [1] Mohammad K, et al. Consensus Approach for Standardizing the Screening and Classification of Preterm Brain Injury Diagnosed with Cranial Ultrasound: A Canadian Perspective. *Front Pediatr*. 2021;9:618236

Preterm brain injury type	GMH-IVH	PVHI	PHVD	cWMI	CBH
Total diagnoses	460	103	65	14	8
Total number of inconsistencies between observers (% of total)	33 (7%)	1 (1%)	8 (12%)	2 (14%)	0
Intra-class correlation coefficient	0.92	0.99	0.92	0.93	1.00

Table showing the total number of injury diagnoses per injury type (counted for both left and right hemisphere for GMH-IVH, PVHI and cWMI) made in the 292 extremely preterm infants with GMH-IVH. Also showing the total number of inconsistencies and agreement in brain injury diagnoses between the 2 observers after consensus approach implementation.

Incidence of brain lesions in moderate-late preterm infants assessed by cranial ultrasound and MRI: The BIMP-study

Boswinkel V^a, Nijboer J, Krüse-Ruijter M^a, Wu-Smit M^a, Mulder-de Tollenaer S^a, Boomsma M^a, de Vries L^{b,c}, **Meijler G^a**

^aIsala, Zwolle, Netherlands

^bWilhelmina Children's Hospital, University Medical Center Utrecht, Utrecht, Netherlands

^cLeiden University Medical Center, Leiden, Netherlands

BACKGROUND/PURPOSE: Moderate-late preterm (MLPT) infants, born at 32 – 36 weeks' gestation, do not routinely undergo neuro-imaging. The aim of this study

was to investigate the incidence and characteristics of brain lesions in MLPT infants using cranial ultrasound (cUS) and magnetic resonance imaging (MRI).

METHODS: Between August 2017 and November 2019, MLPT infants born between 32+0 and 35+6 weeks' gestation were included in a prospective cohort study that was carried out at Isala Women and Children's Hospital, Zwolle, the Netherlands. Neuroimaging was performed at three time points: cUS at postnatal day 3–4 (early-cUS), before discharge and repeated at term equivalent age (TEA). In addition, infants underwent an MRI at TEA. CUS and MRI were scored using a scoring system for abnormalities e.g. hemorrhages, white matter and deep gray matter injury, including mild lesions. Furthermore, brain maturation and gyration were visually evaluated. Brain lesions were classified as mild or moderate-severe. Incidences and confidence intervals were calculated.

RESULTS: In total, 166 MLPT infants participated and underwent cUS. Of these, 127 infants underwent MRI. The overall incidence of mild brain lesions was 71.7% (119/166) and of moderate-severe lesions 3.6% (6/166) on cUS and/or MRI. The most frequent lesions were signs suggestive of white matter injury: inhomogeneous echogenicity in 30.5% (50/164) infants at early-cUS, in 8.1% (12/148) infants at TEA-cUS and diffuse white matter signal changes (MRI) in 25.5% (27/127) infants. On MRI, cerebellar hemorrhage was observed in 12.6% (16/127) infants and delayed maturation in 13.4% (17/117) infants. Small hemorrhages and punctate white matter lesions were better detected on MRI than on cUS.

CONCLUSIONS: Mild brain lesions were frequently encountered in MLPT infants, especially signs suggestive of white matter injury and small hemorrhages. Moderate-severe lesions were less frequently seen.

Resistive index in early onset neonatal sepsis

Mishra A^a, Deshmukh L^a

*^aGovernment Medical College Aurangabad
Maharashtra India, Government Medical College
Aurangabad, India*

BACKGROUND: Cerebral hemodynamics in early onset neonatal sepsis is complex and poorly understood. There is dearth of adequate knowledge in the literature regarding cerebral blood flow (CBF) changes in early onset neonatal sepsis (EONS). The aim of our study was to study CBF by measuring the resistive index (RI) of the anterior cerebral artery in EONS.

METHODOLOGY: All newborn admitted in our intensive care unit having suspicion of EONS during the period of January 2021 to June 2021 underwent point of care transcranial doppler ultrasonography to measure the RI of the anterior cerebral artery within 24hrs of onset of signs and symptoms before starting inotrope if at all recommended. Neonates with congenital malformations,

genetic syndromes, perinatal asphyxia and metabolic disorders were excluded. Babies with positive blood culture were included in the final analysis.

RESULTS: out of 88 suspected EONS, 60 babies were analyzed, of which 25 were culture positive and included in the final study. The mean gestational age was 33.3 ± 2.4 week and the mean birth weight being 1.94 ± 0.77 kg. Most common organism isolated was *Escherichia coli* (72%) followed by *klebsiella pneumoniae* (14%). Lower RI was documented in 52% (13 of 25), normal in 40% (10 of 25) and variable in 8% (2 of 25) cases.

CONCLUSION: In the present study, we have documented a decrease in RI suggestive of increased CBF in EONS. However, a larger scale of data would help in better understanding of the hemodynamics in EONS.

Value of routine magnetic resonance venography for the diagnosis of cerebral venous sinus thrombosis in neonates with encephalopathy receiving therapeutic hypothermia

Munster C^a, Elshibiny H^a, Szakmar E^{a,b}, Yang E^c, Inder T^a, El-Dib M^a

*^aDepartment of Pediatric Newborn Medicine,
Brigham and Women's Hospital, Harvard Medical
School, Boston, United States*

*^b1st Department of Pediatrics, Semmelweis
University, Budapest, Hungary*

*^cDepartment of Radiology, Boston Children's Hospital,
Harvard Medical School, Boston, United States*

BACKGROUND AND PURPOSE: Neonatal encephalopathy (NE) may be associated with increased incidence of cerebral venous sinus thrombosis (CVST), a diagnosis with significant therapeutic implications. A recent study by Radicioni et al. demonstrated that 10 out of 37 asphyxiated neonates (27%) undergoing therapeutic hypothermia (TH) were diagnosed with CVST using magnetic resonance venography (MRV) [1]. For this reason, MRV was routinely added to the imaging protocol for NE infants in a tertiary care center providing TH for neonates with mild, moderate, and severe encephalopathy. We investigated the frequency of CVST diagnoses before and after this change in practice to determine the frequency of CVST and whether routine MRV increased the diagnosis of this entity.

METHODOLOGY: We performed a retrospective chart review for all neonates who received TH from January 2014-March 2020 at Brigham and Women's Hospital. Demographic and clinical data of the study cohort were compared between those who had an MRV and those who did not have one. MRV was routinely performed for cooled neonates with NE between April 2018 and March 2020.

Incidence of CVST detection was compared before and after implementation of routine MRV.

RESULTS: There were 291 babies cooled during the study period. Demographic and clinical characteristics of the study cohort are provided in Table 1. Before the routine use of MRV, there were 209 babies cooled, and 25 (12%) of them had MRV. Only one baby was diagnosed with CVST in this period, and it was initially detected with MRI and then confirmed with MRV. Following the routine inclusion of MRV in the imaging protocol in April 2018, 82 neonates were cooled. Of these 82, 74 (90%) had MRV performed. None of these neonates were diagnosed with CVST. Out of a total of 99 neonates with MRV, 15 showed severe cerebral veins asymmetry. Representative MRI and MRV scans of the infant with CVST and another infant with asymmetry but no CVST are shown in Figure 1. Case 1 demonstrates the importance of intraluminal signal abnormality (T1 and SWI) as well as vessel expansion in diagnosing CVST. While asymmetry of the transverse/

sigmoid sinuses on MRV is a common anatomic variant (Case 2), it might be difficult to differentiate it from CVST in cases with complete absence of flow.

CONCLUSION: Incidence of venous thrombosis in neonates receiving TH for NE may not be as common as previously reported. Routine MRV has not been associated with increased detection of venous thrombosis.

Bibliography:

- [1] Radicioni, M., et al., Cerebral Sinovenous Thrombosis in the Asphyxiated Cooled Infants: A Prospective Observational Study. *Pediatr Neurol*, 2017. 66: p. 63-68.

White matter maturity of female and male extremely preterm neonates - A quantitative MRI study

Schmidbauer V^a, Dovjak G^a, Goeral K^a, Klebermass-Schrehof K^a, Berger A^a, Prayer D^a, Kasprian G^a

^aMedical University Of Vienna, Vienna, Austria

BACKGROUND AND PURPOSE: Former preterm born males are at higher risk for neurodevelopmental disabilities compared to female infants born at the same gestational age (GA) [1]. This study investigated sex-related differences in the maturity of the brainstem and internal capsule regions in infants born before 28 weeks GA, using diffusion-tensor- and relaxometry-based MRI techniques.

MATERIALS AND METHODOLOGY: In this study, quantitative MRI sequence acquisitions were analyzed in a sample of 35 extremely preterm neonates imaged at term-equivalent ages. Quantitative MRI metrics [fractional anisotropy (FA); ADC (10-3mm²/s); and T1-/T2-relaxation time (T1R/T2R) (ms)] of the medulla oblongata, pontine tegmentum, midbrain and the right/left posterior limb of the internal capsule (PLIC) were determined on diffusion-tensor- and multi-dynamic multi-echo (MDME) sequence-based imaging data [2]. For each brain section of interest, two separate ROIs were drawn at different levels (Figure 1). ANCOVA and a paired t-test were used to compare female and male infants and to detect hemispheric developmental asymmetries.

RESULTS: Seventeen female [mean GA at birth: 26+0 (±1+4)] and 18 male [mean GA at birth: 26+1 (±1+3)] infants were enrolled in this study.

Significant differences were observed in T1R of the midbrain between female and male neonates ($p < .001$) (Figure 2). In both sexes, FA [$p(\varphi) < .001/p(\sigma) < .001$], ADC [$p(\varphi) < .001/p(\sigma) < .001$], and T1R [$p(\varphi) < .001/p(\sigma) < .001$] differed significantly between the right and left PLIC.

Table 1: Demographic and clinical data of the cohort

	Total n=291	With MRV n=99	Without MRV n=192	p-value
Sex (male)	165 (56.7%)	56 (56.6%)	109 (56.8%)	1
Gestational age (weeks) ^a	38.9 ± 1.74	38.7 ± 1.8	39.0 ± 1.7	0.44
Apgar 1 min ^b	2 (2-4)	2 (2-4)	2 (1-4)	0.61
Apgar 5 mins ^b	6 (5-7)	7 (5-7)	6 (4-7)	0.34
Apgar 10 mins ^b	7 (6-8)	7 (6-8)	7 (6-8)	0.23
Electrographic seizures	20 (6.9%)	8 (8.1%)	12 (6.3%)	0.63
Stage of NE (n=232)				
Mild	105 (36.1%)	37 (37.4%)	68 (35.4%)	0.28
Moderate	116 (39.9%)	51 (51.5%)	65 (33.9%)	0.18
Severe	11 (3.8%)	5 (5.1%)	6 (3.1%)	0.76
Umbilical Blood Gases				
UA pH (n=226) ^a	7.04 ± 0.14	7.07 ± 0.13	7.03 ± 0.15	0.14
UA BD (n=210) ^a	11.5 ± 4.7	11.3 ± 4.8	11.6 ± 4.6	0.49
UV pH (n=249) ^a	7.12 ± 0.15	7.14 ± 0.13	7.11 ± 0.15	0.35
UV BD (n=240) ^a	10.1 ± 4.4	9.9 ± 4.4	10.2 ± 4.4	0.64
Length of hospital stay (days) ^b	8 (6-13)	9 (6-15)	8 (6-12)	0.09
Death	5 (1.7%)	1 (1.0%)	4 (2.1%)	0.67

Abbreviations: NE, neonatal encephalopathy; UA, umbilical artery; UV, umbilical venous; BD, base deficit

Note: Data are presented as n (%)

^a Mean ± SD

^b Median (Interquartile Range)

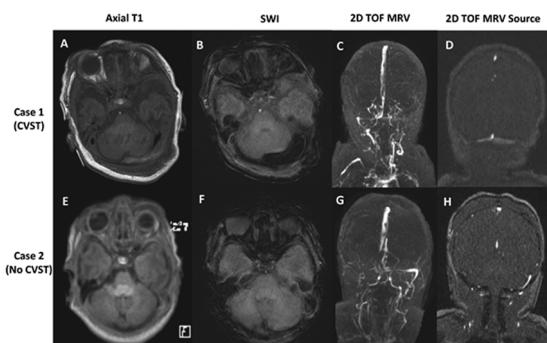
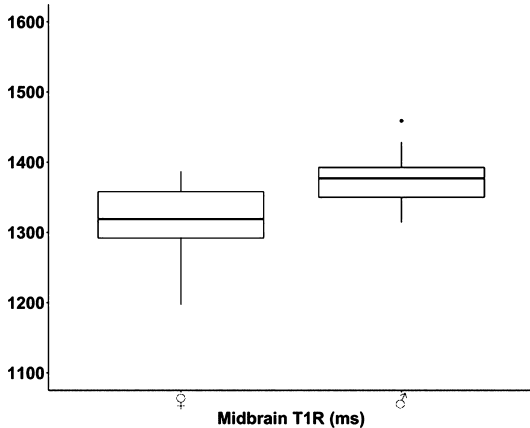
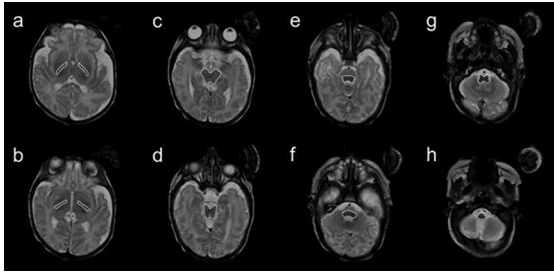


Figure 1: MRI and MRV images of the Case 1 (the baby diagnosed with CVST, panels A-D) and Case 2 (a baby with asymmetry on MRV but no CVST, panels E-H)

Case 1: Demonstration of linear hyperintensity on Axial T1(A) and susceptibility on SWI (B) in the region of the left transverse sinus not associated with significant asymmetry on MRV (C and D)

Case 2: Demonstration of absence of flow in the right transverse and sigmoid sinuses on MRV (G and H) in absence of clear corresponding thrombosis in T1 and SWI sequences (E and F)

Abbreviations: SWI, Susceptibility weighted imaging; TOF, Time of flight



CONCLUSION AND IMPACT: T1R and diffusion-tensor metrics are sensitive markers for the detection of sex-related and interhemispheric differences of white matter maturity. The midbrain of male preterm neonates is more immature compared to female infants at term-equivalent ages. Sex differences in white matter maturation need further attention for the personalization of neonatal brain imaging.

Bibliography:

- [1] Skiöld B, Alexandrou G, Padilla N, et al. Sex differences in outcome and associations with neonatal brain morphology in extremely preterm children. *J Pediatr* 2014;164:1012–1018
- [2] Schmidbauer V, Geisl G, Diogo M, et al. SyMRI detects delayed myelination in preterm neonates. *Eur Radiol* 2019;29:7063–7072

Collaborative curriculum for neonatal neuroradiology conferences

Sewell E^a, Milla S^b, Kadom N^a

^aEmory University; Children's Healthcare of Atlanta, Atlanta, United States

^bChildren's Hospital Colorado, Aurora, United States

PURPOSE: Traditionally, some neonatal intensive care units briefly review neuroimaging cases with a radiologist

on a regular schedule as part of routine clinical care. Additionally, trainees may rotate through radiology as a visitor in the reading room. The trainee education during these experiences can be highly variable and depends on the ability and willingness of the radiologist to engage the trainee, as well as the variety and relevance of cases occurring on any given day. We aimed to create a formal collaborative neuroimaging curriculum between pediatric neuroradiology and neonatal medicine geared towards neonatology fellows that was clinically relevant and reviewed key board concepts.

METHODS AND MATERIALS: This program engages a single pediatric neuroradiologist and neonatologist throughout the fellowship year and focuses on neuroimaging studies in neonates. This curriculum for neonatology fellows was implemented in 2018. Between 7-8 neonatology fellows participate each year. The curriculum consists of four 1-hour sessions throughout the academic year. The American Board of Pediatrics (ABP) Neonatal-Perinatal Medicine board content outline specifications for neuroimaging and neurological disorders were used to create the curriculum.

RESULTS: Fifteen neonatology fellows have participated since the beginning of the program. A total of 12 sessions have been taught to date. The attending time effort per year was 10 hours for the neonatology attending (session case selection, scheduling, session attendance, session feedback review) and 6 hours for the pediatric neuroradiologist (30 min/session case review prior to presentation, session attendance). The curriculum consisted of preparatory reading relevant to the session topic, case studies focusing on key neuroimaging findings, and relevance of imaging to clinical management. The sessions evolved to the following format: (1) head US with focus on preterm brain injury; (2) brain MRI with focus on hypoxic-ischemic encephalopathy; (3) brain MRI with focus on other brain injury in the term infant including stroke and congenital malformations); and (4) fellow case presentations including neuroimaging with attending feedback. Standardized evaluations consisting of Likert scale and open-ended questions were collected intermittently starting in 2019; a sample is provided in Figure 1. A median of 4 evaluations were completed on average for 6 sessions (22 total evaluations). 100% of evaluators agreed or strongly agreed that the sessions delivered important teaching topics and that the presentation was practical and useful. The most common suggested improvement was alterations to the session format.

CONCLUSIONS: ABP certification in Neonatal-Perinatal Medicine requires that neonatology fellows understand the indications and limitations of specific neuroimaging studies and gain competence in interpreting imaging studies and major patterns of injury. Real-life case studies with targeted incorporation of neuroimaging and high-yield neurological disorders are an effective teaching method for adult learners. This knowledge will aid future neonatologists who may practice in hospitals without trained pediatric radiologists.

Neonatal Neuroradiology Conference – 6/18/19 – Drs. Elizabeth Sewell & Sarah Milla

Feedback Form

Please indicate your assessment of the presentation:

1-Strongly Disagree 2-Disagree 3-Neutral 4-Agree 5-Strongly Agree

The presentation had clearly defined objectives:	1	2	3	4	5
The presentation delivered important teaching points:	1	2	3	4	5
The presentation was practical and useful:	1	2	3	4	5
The speaker demonstrated command of the material:	1	2	3	4	5
The speaker had effective tone, pace and delivery	1	2	3	4	5
The speaker engaged the audience effectively	1	2	3	4	5

What did the speaker do well:

1. Explains findings very clearly and in a way that helps me remember them in the future.

2.

What could the speaker have been done better:

1.

2.

What changes would you like made for this conference in the future:

1. I think this is a very helpful conference and have learned a lot from it this past year. I think having each meeting dedicated to a certain topic – i.e. the first meeting being just a review of neuroimaging in general, another meeting dedicated to IVH/bleeds, one dedicated to HIE, etc – and then later in the year a review of everything or other miscellaneous/interesting cases would be great.

Diffusion tensor tractography of the corticospinal tracts in neonates after hypoxic ischemic encephalopathy

Eshel D^a, Shelef I^{a,b}, Abramsky R^{a,c}, Eshel R^{a,d},
Novoa R^{a,b}, Golan A^{a,c}, Marks K^{a,c}, **Shany E**^{a,c}

^aFaculty of Health sciences, Be'er Sheva, Israel

^bRadiology Department, Soroka Medical Center, Be'er Sheva, Israel

^cNeonatal Department, Soroka Medical Center, Be'er Sheva, Israel

^dClinical Research Center, Soroka Medical Center, Be'er Sheva, Israel

BACKGROUND AND PURPOSE: Neonatal Hypoxic Ischemic Encephalopathy (HIE) is a major cause of neurologic disabilities in term neonates. MRI scans of infants who suffered from HIE is commonly used to predict long term neurodevelopmental outcome [1-5]. Diffusion tensor imaging (DTI) is a quantitative MRI technique that measures the magnitude and direction of water molecules movement in a medium which are characterized respectively by the apparent diffusion coefficient (ADC) and fractional anisotropy (FA) [6-8]. Diffusion tensor tractography (DTT) is a validated fiber-tracking method that utilizes DTI generated vectors to visualize and model neuronal fiber tracts within the brain [9,10]

HYPOTHESIS: Cerebral tracts' diffusion parameters are negatively affected by the HIE-related neurological insult and can be used to predict long term neurodevelopmental outcome.

MAIN OBJECTIVE: Evaluate the associations of corticospinal tracts' diffusion values with the degree of MRI brain injury in infants with neonatal HIE. Secondary objectives were to evaluate the associations of the tract's diffusion values with cerebral activity in the first week of life.

METHODOLOGY: Retrospective study of a prospective cohort of infants with neonatal HIE admitted to the Soroka Medical Center NICU between 2014-2020. Included were infants underwent an MRI scan prior to discharge and within the first 10 days of life. Scans were prospectively scored for evidence of brain injury according to the Rutherford et al. severity scoring system that was modified to include a diffusion weighted sequence [11,12]. Explore DTI software [13] streamline deterministic method was used for CST tractography (figure 1). Volume, fractional anisotropy (FA) and apparent diffusion coefficient (ADC) data were extracted. Neonatal data for seizures, abnormal aEEG, abnormal neurologic status at discharge, or death was retrieved.

RESULTS: Sixty-six infants were included in the study with a median gestational age of 40W+1D. Significant association was found between a worse MRI score and a longer stay in the ICU (8 vs. 9 vs. 20, p=0.002), seizures (p=0.012), abnormal aEEG background (p<0.001), abnormal neurologic status at discharge (2.6% vs. 36.4% vs. 55.6%, p<0.001) and death (p=0.001). A significant negative association was found between a higher MRI category score, tract volume and diffusion values (Table 1). These associations remained significant after adjustment for infants' gestational age, age at MRI scan (in days) and aEEG seizures.

CONCLUSIONS: We demonstrated that a decrease in diffusion values: ADC bilaterally and FA on the left side, was significantly associated with a higher likelihood of worse MRI category scores. These findings support a possible prognostic role of the CST tracts diffusion values early after birth. More work is needed in order to assess the association of tracts' diffusion values with long term outcome in neonatal HIE.

Bibliography:

- [1] Twomey E, Twomey A, Ryan S, Murphy J, Donoghue VB. MR imaging of term infants with hypoxic-ischaemic encephalopathy as a predictor of neurodevelopmental outcome and late MRI appearances. *Pediatr Radiol.* 2010;40(9):1526–35.
- [2] Hayes BC, Ryan S, Mearney C, Mulvany S, Doherty E, Grehan A, et al. Brain magnetic resonance imaging and outcome after hypoxic ischaemic encephalopathy. *J Matern Neonatal Med.* 2016;29(5):777–82.

[3] Laptook AR, Shankaran S, Barnes P, Rollins N, Do BT, Parikh NA, et al. Limitations of Conventional Magnetic Resonance Imaging as a Predictor of Death or Disability Following Neonatal Hypoxic-Ischemic Encephalopathy in the Late Hypothermia Trial. *J Pediatr*. 2020 Nov;

[4] Goergen SK, Ang H, Wong F, Carse EA, Charlton M, Evans R, et al. Early MRI in term infants with perinatal hypoxic-ischaemic brain injury: interobserver agreement and MRI predictors of outcome at 2 years. *Clin Radiol*. 2014 Jan;69(1):72–81.

[5] Rutherford MA, Pennock JM, Counsell SJ, Mercuri E, Cowan FM, Dubowitz LM, et al. Abnormal magnetic resonance signal in the internal capsule predicts poor neurodevelopmental outcome in infants with hypoxic-ischemic encephalopathy. *Pediatrics*. 1998 Aug;102(2 Pt 1):323–8.

[6] Mori S, Zhang J. Principles of Diffusion Tensor Imaging and Its Applications to Basic Neuroscience Research. *Neuron*. 2006 Sep;51(5):527–39.

[7] Basser PJ, Mattiello J, LeBihan D. MR diffusion tensor spectroscopy and imaging. *Biophys J*. 1994;66(1):259–67.

[8] Basser PJ, Pierpaoli C. Microstructural and physiological features of tissues elucidated by quantitative-diffusion-tensor MRI. 1996. *J Magn Reson*. 1996;213(2):560–70.

[9] Catani M, Howard RJ, Pajevic S, Jones DK. Virtual in Vivo interactive dissection of white matter fasciculi in the human brain. *Neuroimage*. 2002;17(1):77–94.

[10] Stieltjes B, Kaufmann WE, Van Zijl PCM, Fredericksen K, Pearlson GD, Solaiyappan M, et al. Diffusion tensor imaging and axonal tracking in the human brainstem. *Neuroimage*. 2001;14(3):723–35.

[11] Rutherford M, Ramenghi LA, Edwards AD, Brocklehurst P, Halliday H, Levene M, et al. Assessment of brain tissue injury after moderate hypothermia in neonates with hypoxic-ischaemic encephalopathy: a nested substudy of a randomised controlled trial. *Lancet Neurol*. 2010;9(1):39–45.

[12] Okerefor A, Allsop J, Counsell SJ, Fitzpatrick J, Azzopardi D, Rutherford MA, et al. Patterns of Brain

Injury in Neonates Exposed to Perinatal Sentinel Events. *Pediatrics*. 2008;121(5):906–14.

13) Leemans A, Jeurissen B, Sijbers J, Jones D. ExploreDTI: a graphical toolbox for processing, analyzing, and visualizing diffusion MR data. *Proc 17th Sci Meet Int Soc Magn Reson Med*. 2009;17(2):3537.

Table 1- Multivariable Ordinal Logistic Regression

Variable	Left Side			Right Side		
	Unadjusted	Adjusted (3 IV) ^a	Adjusted (4 IV) ^{ab}	Unadjusted	Adjusted (3 IV) ^a	Adjusted (4 IV) ^{ab}
	OR (95% CI)	OR (95% CI)	OR (95% CI)	OR (95% CI)	OR (95% CI)	OR (95% CI)
Tract Volume (mm ³)	0.526 (0.307-0.901)	0.510 (0.292-0.892)	0.398 (0.212-0.749)	0.613 (0.385-0.975)	0.577 (0.358-0.928)	0.532 (0.325-0.871)
Fractional Anisotropy	0.750 (0.462-1.220)	0.689 (0.419-1.134)	0.715 (0.422-1.213)	0.484 (0.255-0.918)	0.388 (0.193-0.779)	0.425 (0.208-0.871)
ADC (mm ² /s)	0.310 (0.158-0.608)	0.290 (0.139-0.606)	0.265 (0.120-0.585)	0.354 (0.181-0.690)	0.347 (0.166-0.725)	0.347 (0.160-0.749)

^a Adjusted for: Diffusion variable, gestational week at birth and age at MRI (days).
^{ab} Adjusted for: Diffusion variable, gestational week at birth, age at MRI (days) and aEEG/seizures.

Characterization of MRI-defined short-term outcomes for infants evaluated for but not treated with therapeutic hypothermia

Thiim K^a, Lee S^a, Singh E^a, Steele T^a, Elshibiny H^a, Inder T^a, El-Dib M^a

^aBrigham and Women’s Hospital, Boston, United States

BACKGROUND AND PURPOSE: Therapeutic hypothermia (TH) is the standard of care for neonatal encephalopathy (NE).¹ In recent years, many centers, including ours at Brigham and Women’s Hospital (BWH), have broadened their TH treatment criteria to include infants with mild NE. Our protocol uses both evidence of perinatal insult and a quantitative Neonatal Encephalopathy Score (NES) of four or more to decide on TH treatment eligibility. Amplitude integrated EEG (aEEG) is used as an adjunct where only infants with a continuous normal voltage (CNV) are excluded from cooling.² Whether these criteria, inclusive of mild encephalopathy, are capable of screening those with no brain injury who might benefit from TH is unknown. Our primary aim was to evaluate short term MRI outcomes in infants evaluated for TH.

METHODOLOGY: We enrolled infants who were screened for but not treated with TH between April 2019 and August 2021. All brain MRIs were obtained within the first week of life at a BWH in-hospital scanner. Clinical MRI reports were used in this analysis.

RESULTS: Thirty-nine infants enrolled in the study had a mean gestational age of 39.0 ± 1.4 weeks. Their detailed demographic and clinical characteristics are reported in Table 1. Of the 39 infants, 34 (87.2%) had no evidence of acute perinatally acquired hypoxic ischemic brain injury. Of note, three of these infants had evidence of chronic punctate white matter injury, and one infant showed an

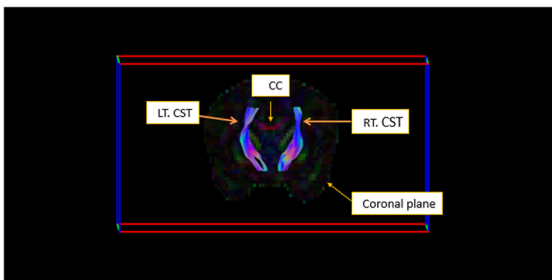


Figure 1- RGB color coded map (Anterior-posterior: green, left-right: red, longitudinal: blue) on the coronal plane of an infant after HIE. Note the longitudinal blue tracts of the CST (delineated by the explore DTI software).

Table 1. Demographical and clinical characteristics of the study cohort (n=39)

	Full Cohort (n = 39)	Infants with injury on MRI (n = 5)
Demographic and Prenatal Data		
GA (wks) *	39.0 \pm 1.4	39.4 \pm 1.7
BW (g) *	3248 \pm 534	3508 \pm 277.8
Sex (% of males)	17 (43.6%)	2 (40%)
Maternal age (yr) *	32.5 \pm 0.5	32.6 \pm 2.2
Sentinel events		
Placenta abruption	3 (7.7%)	0 (0%)
Cord prolapse	1 (2.6%)	0 (0%)
Maternal hemorrhage	2 (5.1%)	1 (20%)
Delivery room and admission data		
C-section	19 (48.7%)	3 (60%)
PPV in DR	21 (53.8%)	4 (80%)
Chest compressions in DR	1 (3.6%)	1 (20%)
Apgar at 1 min *	5 (1-8)	1 (1-7)
Apgar at 5 min *	8 (2-9)	8 (2-9)
UA pH *	7.1 \pm 0.1	7.1 \pm 0.2
UA BD *	10.3 \pm 3.1	9.5 \pm 3.4
UA lactate *	7.8 \pm 1.8	6.1 \pm 2.8
UV pH *	7.2 \pm 0.1	7.3 \pm 0.1
UV BD *	9.3 \pm 2.9	8.9 \pm 3.9
UV lactate *	6.7 \pm 2.1	6.5 \pm 2.8
First hour pH *	7.3 \pm 0.1	7.3 \pm 0.1
First hour BD *	8.6 \pm 3.6	10.1 \pm 4.5
First hour lactate *	6.8 \pm 3.1	8.5 \pm 3.4
Clinical Data		
Highest NE score ^b	2 (0-7)	2 (1-5)
Passive cooling	4 (10.3%)	2 (40%)
Length of stay (d) *	4.7 \pm 5.7	4.0 \pm 1.2

Abbreviations: BD, base deficit; BW, birth weight; DR, delivery room; FHR, fetal heart rate; GA, gestational age; PPV, positive pressure ventilation; UA, umbilical artery; UV, umbilical venous

Note: Data are presented as n (%)

* Mean \pm SD

^b Median (range)

incidental finding of a medullary tumor. Five infants (12.8%) had MRI findings suggestive of acute brain injury displayed by acute diffusion weighted imaging. Three of these cases were small foci of restricted diffusion in the fronto-parietal white matter. The fourth case displayed restriction focally in the left posterior cerebral artery territory. The fifth case displayed acute watershed ischemic injury most notably in the left parieto-occipital lobe. Clinical characteristics of these five cases, along with their MRI findings, are described in Table 2 and displayed in Figure 1. Notably, cases 4 and 5 had normal centro-parietal aEEG on initial evaluation with a posterior injury pattern on MRI.

CONCLUSION(S): These results suggest that the current expanded TH criteria, inclusive of mild NE at a threshold on a systematic neurological examination, is effective at detecting most infants with acute hypoxic ischemic injuries. Notably, two infants with more significant injury displayed a posterior predominant lesion suggesting that clinical exam and aEEG may be less reliable for such focal lesions. Application of neuroimaging in infants considered

Table 2: Detailed characteristics of five cases with acute injuries

Case	Detailed Clinical Characteristics	MRI Findings
1	GA (wks): 36.8 BW (g): 3460 Apgars: 1, 2, 7 PPV in DR: Yes Chest compression in DR: No Sentinel events: None Highest NE score: 1 aEEG: CNV SWC: Present Worst blood gas*: 7.20/9.6/4.5 Hypoglycemia: single episode of asymptomatic hypoglycemia (43mg/dL) at 5 hours treated with dextrose gel x1	<ul style="list-style-type: none"> Single ovoid focus of diffusion restriction with corresponding T2 hypointensity and T1 hyperintensity in the left periaxial white matter. Punctate foci of susceptibility in the dependent portions of the bilateral occipital horns consistent with tiny intraventricular hemorrhage.
2	GA (wks): 39.7 BW (g): 3110 Apgars: 1, 3, 7 PPV in DR: Yes Chest compression in DR: No Sentinel events: None Highest NE score: 5 aEEG: CNV SWC: Absent Worst blood gas*: 7.15/17.6/13.3 Hypoglycemia: No	<ul style="list-style-type: none"> Two tiny foci of decreased diffusivity in the parietal white matter are non-specific.
3	GA (wks): 41.7 BW (g): 3840 Apgars: 7, 9 PPV in DR: No Chest compression in DR: No Sentinel events: None Highest NE score: 1 aEEG: CNV SWC: Absent Worst blood gas*: 6.99/11.9/8 Hypoglycemia: No	<ul style="list-style-type: none"> Foci of T1 shortening and linear T2 hypointensities within the bifrontal white matter with punctate foci of reduced diffusivity. Foci of susceptibility consistent with focal blood products present in the superior left frontal lobe.

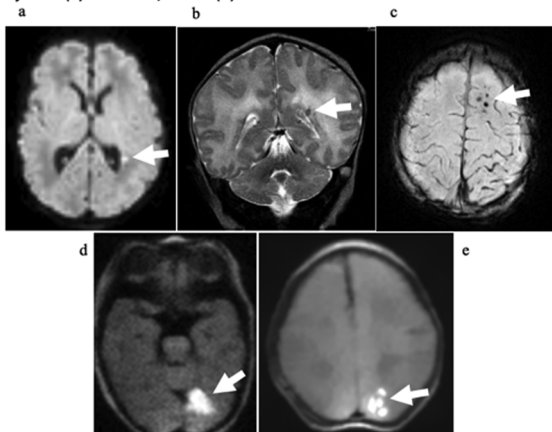
4	GA (wks): 39.4 BW (g): 3690 Apgars: 4, 8, 9 PPV in DR: Yes Chest compression in DR: Yes Sentinel events: Maternal hemorrhage Highest NE score: 2 aEEG: CNV SWC: Present Worst blood gas*: 6.99/11.8/10.1 Hypoglycemia: No	<ul style="list-style-type: none"> • Restricted diffusion and T2 signal abnormality involving left occipital lobe consistent with an infarct in the PCA territory. • Additional small foci of restricted diffusion along the medial left posterior frontal and parietal cortex representing small foci of additional ischemic injury.
5	GA (wks): 39.6 BW (g): 3440 Apgars: 1, 8, 9 PPV in DR: Yes Chest compression in DR: No Sentinel events: None Highest NE score: 3 aEEG: CNV SWC: Absent Worst blood gas*: 7.21/10.3/8.2 Hypoglycemia: No	<ul style="list-style-type: none"> • Multifocal diffusion restriction (approximately 10-15 foci individually less than 1 cm), greatest in the left parieto-occipital lobe where there is a cluster of 5-10 such lesions. This pattern is compatible with acute perfusional ischemic injury or venous congestive injury (12 hours-7 days).
Abbreviations: GA, gestational age; BW, birth weight; PPV, positive pressure ventilation DR, delivery room; NE, neonatal encephalopathy; SWC, sleep-wake cycling *Lowest pH/highest BD/highest lactate. Includes arterial umbilical, venous umbilical, and baby gas within 1 hour		

for cooling but not receiving treatment remains worthy of consideration.

Bibliography:

- 1) Jacobs SE, Berg M, Hunt R, Tarnow-Mordi WO, Inder TE, Davis PG. Cooling for newborns with hypoxic ischaemic encephalopathy. The Cochrane database of systematic reviews. 2013;1:CD003311.
- 2) Brigham and Women's Hospital TH Clinical Practice Guidelines. <https://www.brighamandwomens.org/assets/BWH/pediatric-newborn-medicine/pdfs/th-cpg-amended.pdf>

Figure 1. MRI images of the five cases (from Table 2) with acute injuries: (a) Axial DWI, case 1 (b) Coronal



T2, case 2 (c) Axial SWI, case 3 (d) Axial DWI, case 4 and (e) Axial DWI, case 5. Abbreviations: DWI, diffusion-weighted imaging; SWI, susceptibility-weighted imaging

Investigating functional connectivity in the newborn brain cot-side using wearable high-density diffuse optical tomography

Uchitel J^{a,c}, Blanco B^b, Collins-Jones L^c, Porter E^d, Edwards A^d, Cooper R^c, Austin T^d

^aDepartment of Paediatrics, University of Cambridge, Cambridge, United Kingdom

^bDepartment of Psychology, University of Cambridge, Cambridge, United Kingdom

^cDOT-HUB, Department of Medical Physics and Biomedical Optics, University College London, London, United Kingdom

^dNeonatal Intensive Care Unit, Rosie Hospital, Cambridge NHS Foundation Trust, Cambridge Biomedical Campus, Cambridge, United Kingdom

BACKGROUND/OBJECTIVE: Sleep is an important biomarker of brain development for newborn infants. Newborn infants possess two sleep states: active sleep (AS) and quiet sleep (QS). Like sleep, functional brain connectivity (FC) is tightly linked to brain development, yet the relationship between sleep and FC is poorly understood [1]. This relationship is difficult to investigate using traditional neuroimaging approaches, which often require sedation and cannot be performed cot-side. This study aimed to 1) investigate FC in newborn infants across infant sleep states using high-density diffuse optical tomography (HD-DOT) and 2) demonstrate the utility of a new generation of modular wearable HD-DOT for non-

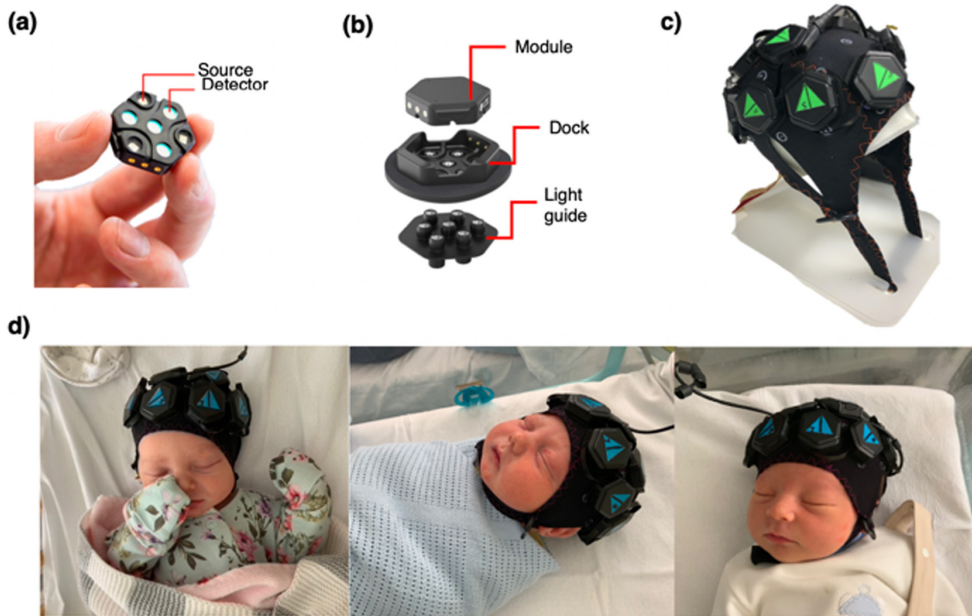


Figure 1. Wearable HD-DOT for cot-side functional imaging of the newborn brain. a) LUMO module with 3 near-infrared light sources and 4 light detectors. b) LUMO modules fit into docks, which then connect to light-guide pieces. c) The cap containing 12 LUMO tiles arranged to cover the frontal and parietal cortices. 12 tiles includes 36 sources and 48 detectors with wavelengths at 735 and 850 nm providing approximately 1700 channels per wavelength, of which ~ 400 fall within 10-60 mm range and thus potentially provide viable signals. The colored high-contrast triangular labels are used to support subject-specific 3D structured illumination surface scanning. This is used to determine the precise location of the cap on the head and the underlying brain areas that the system was sensitive to. d) Three newborn infants in their cots wearing the HD-DOT cap during sleep.

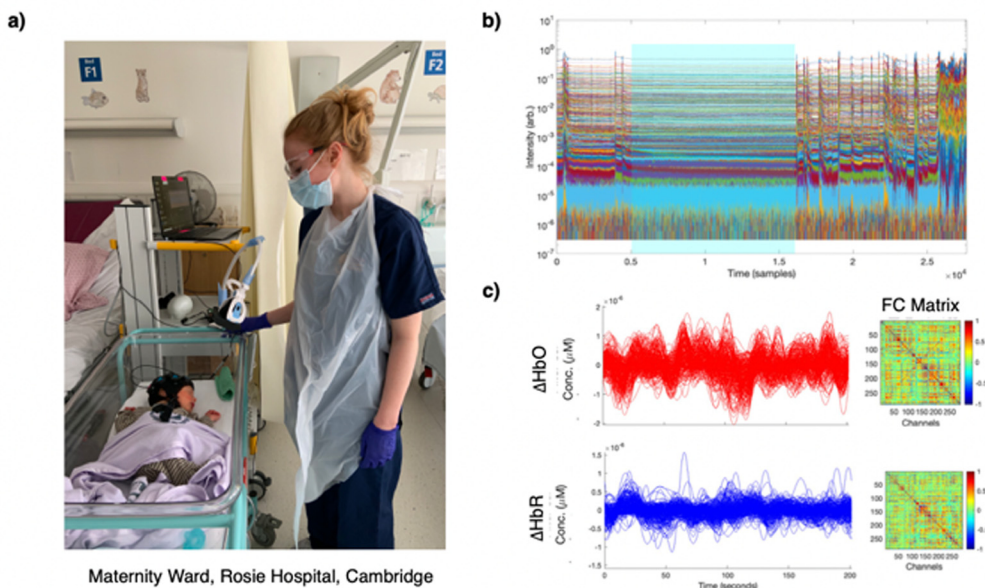


Figure 2. Cot-side HD-DOT recording and HD-DOT data processing. a) All studies were performed cot-side in the maternity ward of the Rosie hospital under COVID-19 conditions. Recordings lasted for 1 hour during which the infant wore the HD-DOT cap and remained asleep. b) Example HD-DOT recording from 1 infant. Motion during sleep is visible as spikes in the signal. c) After recording, data is pre-processed to time series of changes in oxygenated hemoglobin (HbO) and deoxygenated hemoglobin (HbR). Functional connectivity (FC) matrices on the right are computed as the correlation between all channel pairs. Warm colors indicate positive correlations between channel pairs.

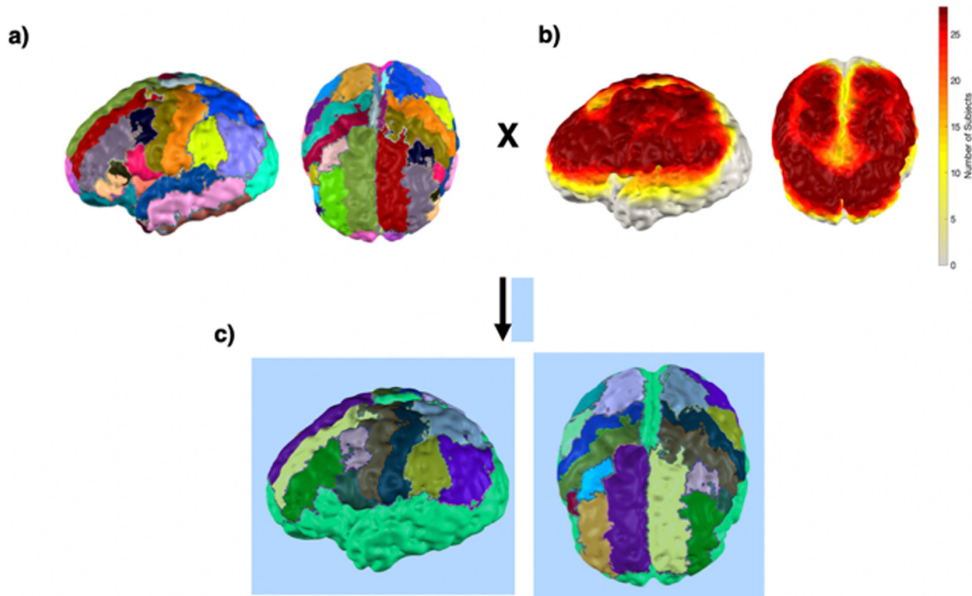


Figure 3. Parcellation of the neonatal cortical surface. Higher-level HD-DOT data analysis are performed in the image space on three-dimensional head models. However, computing functional connectivity (FC) matrices based on high-density head models is computationally expensive. To reduce the dimensionality of this data, a cortical parcellation approach was used. **a)** A neonatal head model's grey matter surface mesh was divided into smaller regions, called parcels. We chose to use the Melbourne Children's Regional Infant Brain atlas (Alexander *et al.*, *Neuroimage*, 2017) for our parcellation scheme, which we felt had the best anatomical specificity as compared to other available newborn infant atlas. We multiplied the sensitivity our HD-DOT array **(b)** by this parcellation to produce a spatial map of the cortical parcels that our system was sensitive to **(c)**. This map was then used to reconstruct HbO and HbR data.

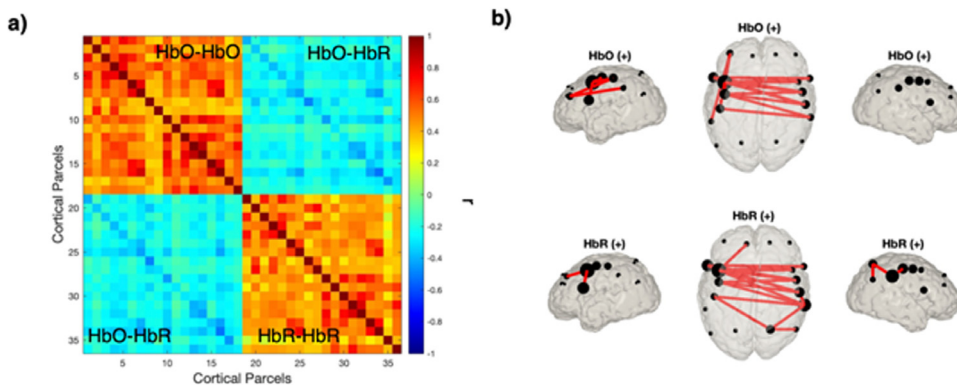


Figure 4. Preliminary results from functional connectivity analyses. **a)** Group-level functional connectivity (FC) matrix computed from individual subjects' FC matrices during quiet sleep. Expected correlation of each chromophore with itself (upper left and bottom right corners) and anticorrelation between HbO and HbR (upper right and bottom left corners) is visible. **b)** Connectome-based independent component analysis (connICA) was used to compute spatial maps of significant connections during quiet sleep. Apparent interhemispheric connectivity supports that our system is capable of capturing FC networks in the newborn infant cot-side.

invasive, cot-side brain imaging in clinical settings.

METHODS: We applied a 12-module wearable HD-DOT system (LUMO, Gowerlabs Ltd.) to study 45 healthy term-born newborn infants during natural sleep (Fig. 1). Video recording of behavior was taken for scoring of sleep state. Three-dimensional structured-illumination images of the head surface were also taken for identification of cranial landmarks, source, and detector positions. A

common neonatal head model was registered to these positions, resulting in a 3D mesh model for each subject. From recordings, clean data segments that were at least 3 mins in duration were extracted and preprocessed (Fig 2). Preprocessed data segments were then reconstructed to produce cortical surface images of changes in oxygenated and deoxygenated hemoglobin (HbO and HbR) concentrations. In this image space, HbO and HbR data

were parcellated using the neonatal M-CRIB atlas [2] to reduce data dimensionality and determine the underlying brain regions that the system was sensitive to (Fig. 3). Group-level functional connectivity matrices and connectome-based independent component analysis (connICA) [3] were computed based on parcellated data to further explore the presence of FC.

RESULTS: Of the 45 infants, 28 had at least one clean data segment (62% subject retention rate) of at least 3 mins (mean: 5.2 ± 3.0). Of the 63 segments, 18 were during AS (mean: 4.2 ± 1.1 min), 40 were QS (mean: 5.6 ± 3.7 min), and 4 were in transitional sleep. Group-level functional correlation matrices using these segments also support the presence of FC in this dataset given strong correlation between HbO-HbO and HbR-HbR (Fig. 4). Preliminary connICA analysis of data during quiet sleep demonstrates the presence of significant interhemispheric connectivity (Fig. 4).

CONCLUSION: Preliminary results support that HD-DOT is a suitable and well-tolerated method to obtain high-quality FC data in newborn infants in clinical settings. Additional higher-level analyses currently underway are spatial independent component analysis (spatial ICA), network-based statistics, and statistically comparing FC features across AS and QS. Pilot studies of this system on preterm infants are also currently underway using an 8-module LUMO system.

[1] Lee et al., *Front. Neurosci.*, 2020

[2] Alexander et al., *Neuroimage*, 2017

[3] Amico et al., *Neuroimage*, 2017.

Improved segmentation of neonatal brain MRI scans by addressing motion artifacts with data interpolation

Verschuur A^{a,b}, Boswinkel V^{c,d}, Tax C^{b,e}, van Osch J^a, Nijholt I^a, Slump C^f, de Vries L^{g,h}, van Wezel-Meijler G^c, Leemans A^b, Boomsma M^a

^aDepartment of Radiology, Isala Hospital, Zwolle, Netherlands

^bImage Sciences Institute, University Medical Centre Utrecht (UMCU), Utrecht, Netherlands

^cDepartment of Neonatology, Isala Women and Children's Hospital (IVKC), Zwolle, Netherlands

^dUMC Utrecht Brain Center, University of Utrecht, Utrecht, Netherlands

^eCardiff University Brain Research Imaging Centre, Cardiff, United Kingdom

^fDepartment of Robotics and Mechatronics, University of Twente, Enschede, Netherlands

^gDepartment of Neonatology, Wilhelmina Children's Hospital, Utrecht, Netherlands

^hDepartment of Neonatology, Leiden University Medical Centre (LUMC), Leiden, Netherlands

BACKGROUND: Motion artifacts are a common problem in neonatal brain MRI and may negatively affect segmentation. The purpose of this study was to investigate whether motion-affected slices can be replaced by

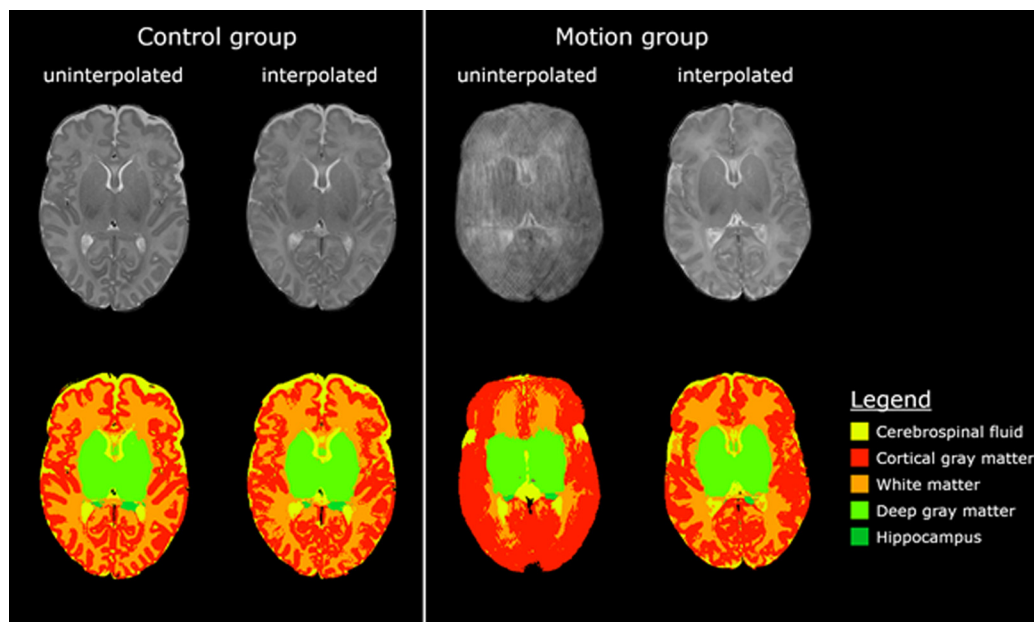


Figure 1: Interpolation and segmentation results of scans in the control and motion group. The left part of the figure shows one motion-free MRI slice and its corresponding segmentation results before and after interpolation. The right part of the figure shows one motion-affected MRI slice and its corresponding segmentation results before and after interpolation.

interpolated slices to enhance segmentation of neonatal brain MRI scans.

METHODS: From August 2017 to November 2019, moderate-late preterm infants were enrolled in a prospective cohort study entitled Brain Imaging in Moderate-late Preterm infants (BIMP-study). Around term equivalent age, MRI of the brain was performed using a 3 Tesla MRI. T2-weighted (voxel size 0.35x0.35x2mm) transverse images were automatically segmented into eight brain structures with a neonatal segmentation toolbox [1]. Upon visual inspection, scans with motion artifacts that affected segmentation (25/112; motion group) and scans without motion artifacts (27/112; control group) were selected and used for analysis. Slices with motion artifacts were re-estimated using shape-preserving cubic spline interpolation [2, 3], followed by automatic segmentation of the interpolated scan. Analysis was performed in three stages. Firstly, scans from the control group were used to test interpolation reliability: 18/54 axial slices of these scans were interpolated. Segmentation results of uninterpolated and interpolated scans were compared using the Sørensen-Dice coefficient. Secondly, uninterpolated and interpolated volumes of the motion group were compared using the Wilcoxon Signed-Ranks test. Thirdly, interpolated volumes of the motion group were compared to uninterpolated volumes of the control group using the Mann-Whitney U test.

RESULTS: In the control group, Sørensen-Dice coefficients ranged between 0.87 and 0.97. In the motion group, interpolation resulted in a significant decrease of cortical ($Z=-2.9$, $p=0.004$) and deep gray matter ($Z=-3.30$, $p<0.001$), and a significant increase of white matter ($Z=2.84$, $p=0.005$) volumes. No significant differences were found between interpolated volumes of the motion group and uninterpolated volumes of the control group.

CONCLUSION: Shape preserving cubic spline interpolation enables reliable segmentation of motion-affected MRI scans in moderate-late preterm infants.

References:

- [1] Beare RJ, Chen J, Kelly CE, et al. Neonatal Brain Tissue Classification with Morphological Adaptation and Unified Segmentation. *Front Neuroinform* 2016;10:12. DOI:10.3389/fninf.2016.00012.
- [2] Wolberg G, Alfy I. Monotonic Cubic Spline Interpolation. *Proceedings Computer Graphics International* 1999:188-195. DOI: 10.1016/S0377-0427(01)00506-4 .
- [3] Fritsch FN, Carlson RE. Monotone Piecewise Cubic Interpolation. *SIAM J Numer Anal* 1980;17(2):238-246. DOI:10.1137/0717021.

Mild brain lesions do not affect brain volumes in moderate-late preterm infants

Boswinkel V^{a,b}, **Verschuur A**^{c,d}, Nijholt I^c, van Osch J^c, Nijboer-Oosterveld J^c, Beare R^{e,f}, Slump C^g, de Vries L^{h,i}, Boomsma M^e, van Wezel-Meijler G^a

^aDepartment of Neonatology, Isala Women and Children's Hospital (IVKC), Zwolle, Netherlands

^bUMC Utrecht Brain Center, University of Utrecht, Utrecht, Netherlands

^cDepartment of Radiology, Isala Hospital, Zwolle, Netherlands

^dImage Sciences Institute, University Medical Centre Utrecht (UMCU), Utrecht, Netherlands

^eMurdoch Children's Research Institute, The Royal Children's Hospital, Melbourne, Australia

^fDepartment of Medicine, Monash Medical Centre, Monash University, Melbourne, Australia

^gDepartment of Robotics and Mechatronics, University of Twente, Enschede, Netherlands

^hDepartment of Neonatology, Wilhelmina Children's Hospital, Utrecht, Netherlands

ⁱDepartment of Neonatology, Leiden University Medical Centre (LUMC), Leiden, Netherlands

BACKGROUND: The influence of frequently occurring mild brain lesions on brain volumes in moderate (MP; 32+0-33+6 weeks' gestation) and late (LP; 34+0-35+6 weeks' gestation) preterm infants is unknown. The purpose of this study was to investigate the effect of mild brain lesions on brain volumes in moderate-late preterm (MLPT) infants and to compare brain volumes between MP and LP infants.

METHODS: Eligible MLPT infants born in Isala Women and Children's Hospital were enrolled in a prospective cohort study (Brain Imaging in Moderate-late Preterm infants 'BIMP-study') between August 2017 and November 2019. Term equivalent age MRI was performed using a 3T MRI system. MRI scans were assessed for brain lesions by three investigators in consensus. Automatic segmentation of eight brain structures was performed using T2-weighted images and an adapted version of MANTiS (Morphologically adaptive neonatal tissue segmentation toolbox). Absolute and relative

Table 1. Population Demographics and Clinical Characteristics

Variables	NT Group	NA Group	p-value
Female Gender	7/13 (53.9%)	8/14 (57.1%)	1.00
Gestational Age (weeks)	39.6 (39.0-40.6)	39.0 (38.0-39.6)	0.52
Birth Weight (g)	3310 (3050-3800)	3283 (3025-3700)	0.80
Head circumference (cm)	34.5 (33.0-36.0)	34.3 (33.5-35.5)	0.57
Length of NICU stay (days)	7.0 (6.0-10.0)	9.5 (6.0-13.0)	0.45
Age at scan (days)	4.0 (4.0-4.0)	2.0 (0.0-4.0)	0.04
Age at follow-up (months)	21.4 (18.8-24.0)	20.8 (18.9-22.3)	0.89
Maternal age (years)	34.0 (33.0-38.0)	31.5 (26.0-35.0)	0.09

(proportion of intracranial volume) brain volumes were compared between infants with and without mild brain lesions and between MP and LP infants using linear regression analysis. Analyses were adjusted for postmenstrual age and weight at MRI. Statistical significance levels were set at $p < 0.05$.

RESULTS: In total, 104 infants were included in this part of the BIMP-study (68 with and 36 without mild brain lesions; 36 MP and 68 LP). Univariate analyses showed significantly larger intracranial ($B=27.4\text{cm}^3$, $p=0.02$),

cerebrospinal fluid ($B=8.78\text{cm}^3$, $p=0.01$) and cerebellar volumes ($B=1.70\text{cm}^3$, $p=0.03$) in infants with mild brain lesions compared to infants without mild brain lesions. Multivariate analyses were not significant. Mean brain volumes were larger in LP infants compared to MP infants, but differences were not significant. Relative brain volumes were not significantly different in both analyses. **CONCLUSION:** Neither having mild brain lesions, nor being born moderately prematurely has a significant effect on brain volumes at term equivalent age in MLPT infants.